Adv. Polar Upper Atmos. Res., **17**, 60–76, 2003

SC-related kilometric and hectometric radiations observed by the Akebono satellite in the polar regions

Atsuki Shinbori[1], Takayuki Ono[1], Masahide Iizima[1], Atsushi Kumamoto[1] and Hiroshi Oya[2]

[1] *Department of Geophysics, Graduate School of Science, Tohoku University, Sendai 980-8578*
[2] *Fukui University of Technology, Fukui 910-8505*

(Received January 6, 2003; Accepted May 27, 2003)

Abstract: Plasma wave phenomena associated with sudden commencements (SCs) were analyzed using the database of Akebono satellite observations that has been contributed to for more than 13 years, since March 1989. The plasma wave data from 263 satellite passages covering the onsets of SCs included 85 cases of auroral kilometric radiation (AKR) enhancement within a frequency range of 100 kHz to 1.2 MHz. The majority of the spectra of the SC-related AKR exhibited a two-banded structure with a harmonic relationship. The start time of the AKR enhancements tended to occur after the onset of the SCs, determined using the geomagnetic records of the Kakioka Magnetic Observatory, within a time range of 3 to 8 min, with an average delay time of 5.26 min. Based on this delay time feature, the magnetic disturbances associated with SCs were thought to propagate from the dayside magnetosphere to the nightside tail region where they compressed the plasma sheet. On the other hand, the data set reveals 19 cases of terrestrial hectometric radiation (THR) that were also associated with SCs appearing within a frequency range of 900 kHz to 4 MHz. The THR onset tended to occur 1 to 9 min after the SC onset, with an average delay time of 5.84 min.

key words: SC triggered substorm, AKR, THR, delay time

1. Introduction

Sudden changes in solar wind pressure associated with shocks and hydromagnetic discontinuity are well known to compress or decompress the magnetosphere. The magnetic signatures of this phenomenon are clearly identifiable as a sudden commencement (SC) on magnetometer records obtained on the ground as well as on satellites (*e.g.* Araki, 1994). As summarized by Joselyn and Tsurutani (1990), SCs that are followed by geomagnetic storms are known as storm sudden commencements (SSC). The subsequent geomagnetic disturbance is interpreted as the successive onsets of substorms resulting from the interplanetary magnetic field (IMF) being directed southward behind the interplanetary shock wave or discontinuity. If the IMF remains northward behind the shock wave or discontinuity, the SC will not be followed by a geomagnetic storm. Such an SC is known as a sudden impulse (SI). However, the physical mechanisms resulting in SSC and SI are identical.

Several reports on SC-triggered substorm phenomena have been made (*e.g.* Schieldge and Siscoe, 1970; Ullaland *et al*., 1970; Kawasaki *et al*., 1971; Burch, 1972; Kokubun *et al*., 1977; Akasofu and Chao, 1980; Iyemori and Tsunomura, 1983; Baumjohann, 1986). Iyemori and Tsunomura (1983) reported a delay time of about 10 min and regarded this delay as the result of propagation effects in the magnetosphere, based on the analysis of Pi2 data. They also pointed out the possibility that SCs might cause plasma sheet compression. Wilken *et al.* (1986) mentioned that the hydromagnetic waves generated by the encounter of a solar wind shock wave and the magnetopause could affect the distribution of magnetospheric particles and fields as a result of the compression. The redistribution could provide conditions suitable for the generation of a substorm or could even actively trigger a substorm.

Auroral kilometric radiation (AKR) was characterized by Gurnett (1974) as an intense radio emission generated along the auroral field lines and associated with a discrete auroral arc. AKR is presently used as an indicator of magnetic disturbances, such as substorms. However, only a few studies have investigated AKR phenomena related to SC-triggered substorms using satellite measurements. Gail and Inan (1990) reported five cases of AKR that suddenly appeared in the DE-1 satellite data covering the frequency range of 80–400 kHz and that were associated with SCs with a delay time of approximately 2 to 5 min. Wilson *et al.* (2001) reported a CRRES satellite observation case study of an SC event that occurred at 1635 (UT) on July 8, 1991. They showed the sudden appearance of AKR waves together with an intensification of the electromagnetic whistler mode and electron cyclotron harmonic (ESCH) waves associated with the SC. However, detailed statistical analyses were deferred because of the limited numbers of SC-related AKR events in the DE1 and CRRES observations.

In the polar regions, another type of electromagnetic radio emission, known as terrestrial hectometric radiation (THR), has been discovered using observations obtained by the Ohzora satellite (Oya *et al*., 1985). Oya *et al.* (1985) pointed out that the lower cut-off frequency of the THR waves coincided with the plasma frequency of the source regions in the polar ionosphere. Later, observations made using the Akebono satellite showed that diffuse-type THR waves appear in a wide frequency range of 700 kHz to 3.2 MHz (Oya *et al*., 1990; Oya, 1991). However, the generation mechanism and detailed characteristics of the THR waves associated with magnetic disturbances, such as SCs and substorms, have not yet been clarified in detail.

The generation, modification and intensification of plasma waves in the ULF-VLF ranges associated with SCs have been mainly studied using the ground-based observation data (Tepley and Wentworth, 1962; Morozumi, 1965, 1966; Hayashi *et al*., 1968; Hirasawa, 1981; Gail *et al*., 1990). A recent data analysis of long-term Akebono satellite observations has shown that plasma waves are enhanced with a one-to-one correspondence with SCs over the entire polar and plasmasphere regions (Shinbori *et al*., 2002). The onset of SC-related VLF plasma waves was shown to have a delay or lead time within a time range of ± 90 s, compared with the onset of SCs identified using the geomagnetic records of Kakioka Magnetic Observatory.

In this paper, AKR enhancements and THR waves associated with SCs were studied using plasma wave data for the high frequency (Oya *et al*., 1990) and VLF ranges (Kimura *et al*., 1990) from a 13-year database of Akebono satellite observations.

Within the high latitude (Mlat $>45^\circ$) orbital passages of the Akebono satellite, 162 paths covered the simultaneous observation of a ground-based SC. In 85 of the 162 high-latitude SC events, AKR enhancements associated with the SC onsets were identified. Furthermore, in 19 of the 162 high-latitude SC events, THR wave enhancements waves with an intense narrow-band spectrum were seen. For the 101 low-latitude SC events; however, the location of the Akebono satellite inside the plasmasphere (Mlat $<45^\circ$) meant that the AKR waves were seldom observed because of the shielding effect of the plasmasphere and the propagation features of AKR. Thus, SC-related AKR phenomena were not observed for the 101 low-latitude SC events. The purpose of this paper was to clarify the statistical relationship between the SCs and these electromagnetic radiations using the long-term satellite database containing the Akebono satellite observation data sets.

2. Observation data

Observations using the Akebono satellite have been continuously made for more than 13 years since its launch on February 21, 1989, when the satellite was placed in a semi-polar orbit with an inclination of 75° and an initial apogee and perigee of 10500 km and 274 km, respectively. For the present study, the plasma wave data provided by the PWS (in the frequency range of 20 kHz–5.1 MHz) (Oya *et al*., 1990) and VLF (in the frequency range of 3.16 Hz–17.8 kHz) (Kimura *et al.,* 1990) instruments onboard the Akebono satellite were analyzed together with low-energy particle data obtained by the LEP (Mukai *et al*., 1990) instrument, which is also installed onboard the Akebono satellite. The time resolution of the dynamic PWS spectra is 2 s, while the time resolution of the VLF, ELF and LEP data is 8 s, according to the Akebono satellite database.

Within the period from March 1989 to November 2002, 930 SC events were identified in terms of the SYM-H index (Iyemori and Rao, 1996) and the SC definition of Shinbori *et al.* (2002). For each SC event, we used the onset time of the ground-based SC at Kakioka, defined by Shinbori *et al.* (2002). Within the thirteen-year period of Akebono satellite operation from March 1989 to January 2002, 263 cases of plasma wave observations were found to cover the SC onset times. In 85 of the 263 observations, AKR waves were found to be associated with the SC onsets; all of these observations had a delay time of several minutes after the SC onsets in a frequency range of 100 kHz to 1.0 MHz. Furthermore, in 19 of the 263 SC events, THR waves were also found with a delay time of several minutes after the SC onsets in a frequency range of 900 kHz–3.7 MHz.

3. Observations of SC-related AKR in the polar region

3.1. Example case observed on December 24, 1995

An example of an AKR enhancement associated with an SC that occurred at 0600:13 (UT) on December 24, 1995, is given in Fig. 1, which shows the Akebono satellite observations that were made at 6780 km (ALT), 1503 (MLT) and 73.2° (ILAT) near the cleft region. About 7 min after the onset of the SC on the ground, a clear

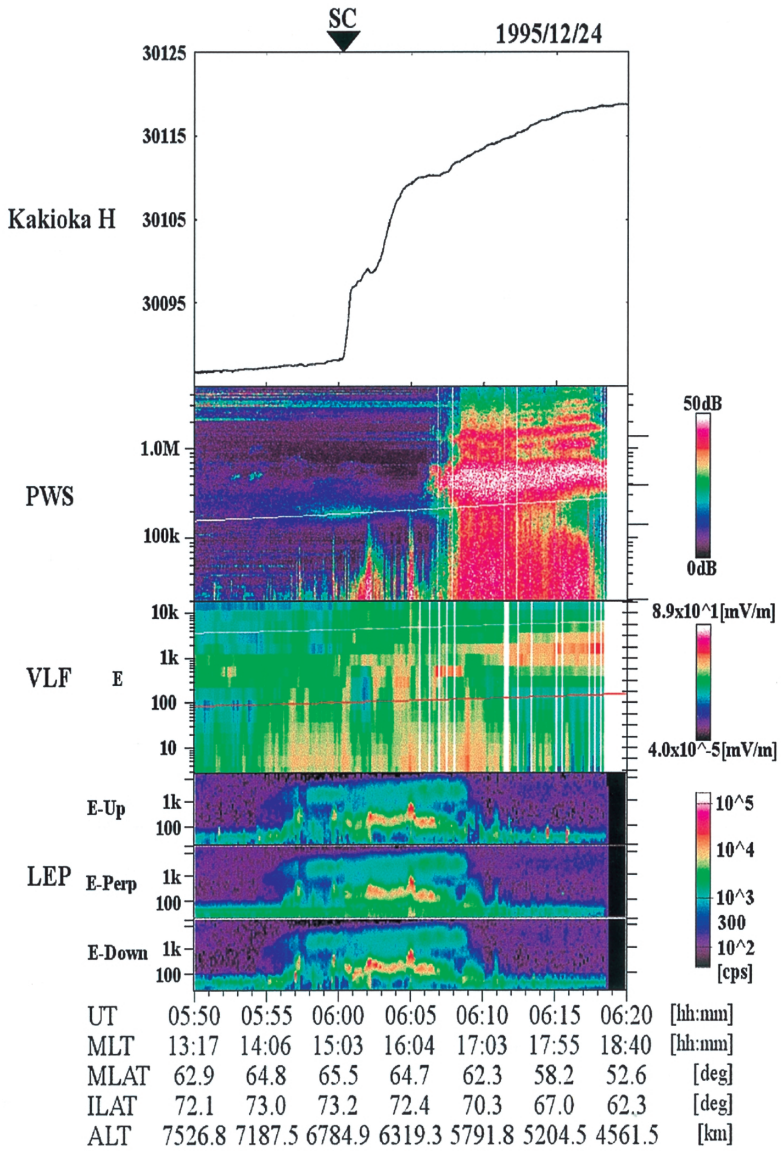

Fig. 1. Dynamic spectra of PWS and VLF plasma waves and the energy-time spectra of low energy particles for three pitch angles observed by the Akebono satellite on December 24, 1995, that were associated with the SC observed at 0600:13 (UT). The top panel shows the geomagnetic data provided by Kakioka observatory; the second panel shows the PWS electric field plasma wave spectrum from 20 kHz to 5.1 MHz, where the white line indicates the electron cyclotron frequency the third shows the VLF electric field plasma wave spectrum from 3.16 Hz to 17.8 kHz where the white and red lines indicate the LHR and proton cyclotron frequencies, respectively. The fourth to sixth panels show the LEP data of electrons for pitch angles of three sectors and an energy range of 10 eV to 16 keV. In the LEP spectra, 'E-Up', 'E-Perp', and 'E-Down' indicate the electron spectra for pitch angle ranges of 0°–60°, 60°–120°, and 120°–180°, respectively. AKR waves suddenly appeared about 7 min after the SC onset.

enhancement of the plasma waves in a frequency range of 200 kHz to 700 kHz suddenly appeared in the PWS dynamic spectrum above the electron cyclotron frequency. Based on the propagation mode, which can be recognized as electromagnetic waves, the plasma waves were identified as AKR. The enhancement of the AKR intensity was sustained until the end of the satellite's passage through the polar regions. The occurrence of the AKR suggests that high-energy electrons precipitated into the auroral regions (Green *et al*., 1979) in association with SC disturbance with a delay time of about 7 min. The spectral intensity and frequency range of the AKR caused by the SC-triggered substorm show the same characteristics as AKR caused by other substorms.

On the other hand, plasma wave enhancements were simultaneously observed with the SC in a wide frequency range of 562 Hz to 90 kHz, as shown in the panels depicting the electric field component of the VLF and PWS data in Fig. 1. As previously reported by Shinbori *et al.* (2002), the enhancement of the electrostatic whistler mode waves began at 0559:37 (UT) with 36 s of lead time before the onset of SC. At the same time as the enhancement of the whistler mode waves, the plasma waves that appeared within a frequency range from the proton cyclotron to the lower hybrid resonance (LHR) frequencies prior to the ground-based SC were also enhanced in these modes, as shown in the panel depicting the electric field component of the VLF range with a banded structure in a frequency range of 562 Hz to 1.78 kHz. These plasma waves can be recognized as proton cyclotron harmonic waves, as shown by Kasahara *et al.* (2001). The impedance of the electrostatic whistler mode waves was about 3000 Ω. This value is larger than that of electromagnetic waves in vacuum (360 Ω). Thus, the waves have an electrostatic nature. On the other hand, the impedances of the proton cyclotron waves and ELF plasma waves were about 200–300 Ω and 100 Ω, respectively. Since these values are smaller than that of the electromagnetic waves in vacuum, these plasma waves have an electromagnetic nature. These results show that the enhancement of the SC-related electrostatic whistler mode waves occurred with a time difference on the order of ten seconds, while the delay times for the appearance of the SC-related AKR phenomena were on the order of minute. In the LEP data, the electron fluxes had been enhanced since 0555 (UT); however, further enhancement associated with the SC and the SC-triggered whistler mode plasma wave phenomena mentioned above was also seen. The enhancement of the electron fluxes continued for about 10 min and suddenly ceased at 0610 (UT). Interestingly, this change in the activity of the electrons' spectra coincides with the start of the AKR.

3.2. Example case observed on August 1, 1990

An example of high-latitude plasma waves associated with an SC that occurred at 0741:07 (UT) is shown in Fig. 2, which displays the Akebono observations made at 4538 km (ALT), 1635 (MLT) and -73.14° (ILAT). At 0740:33 (UT), the enhancement of the plasma waves started within a frequency range of 10 kHz to 140 kHz, as shown in the panels depicting the PWS and VLF data, that is, 34 s before the onset of the SC. These plasma waves were characterized as electrostatic whistler mode waves. The impedance of the ratio of electric and magnetic field intensities of the plasma waves indicated an electrostatic nature. At almost the same time as the enhancement of the electrostatic whistler mode waves, a clear enhancement of the plasma waves within a

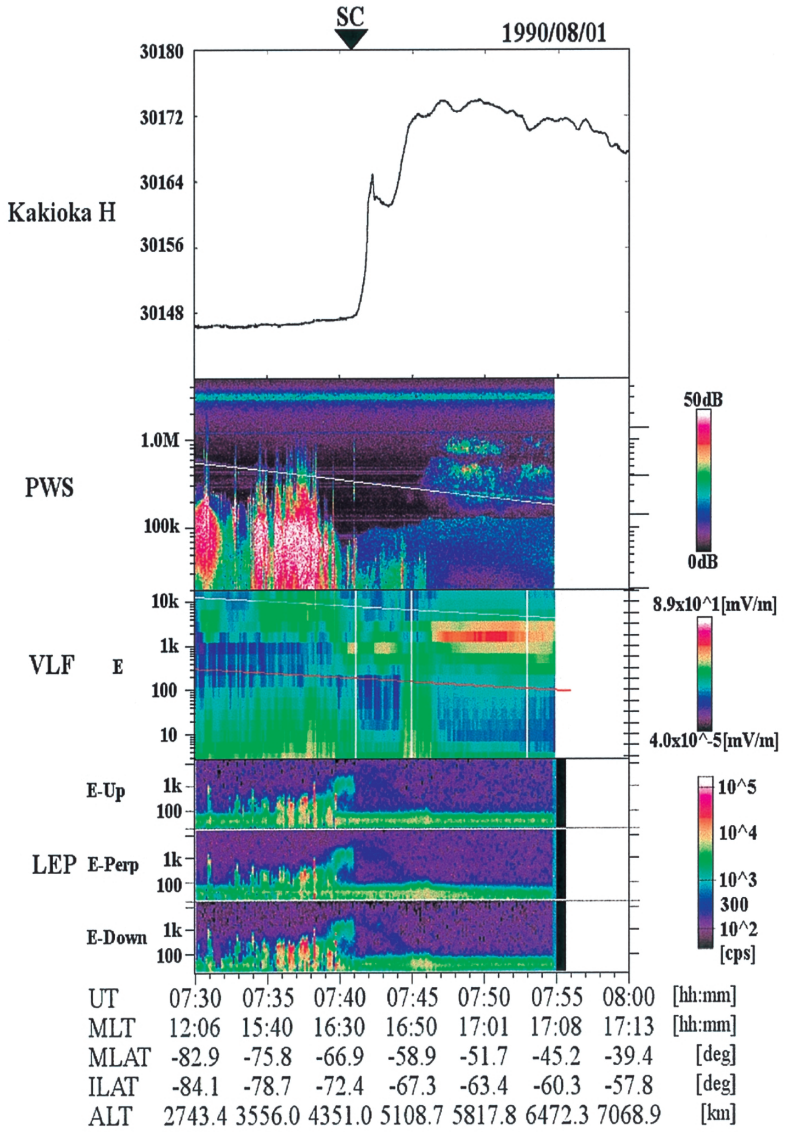

Fig. 2. An example of an SC event that occurred at 0951:11 (UT) on August 1, 1990, when the Akebono satellite passed through the dayside polar region. The formats are the same as in Fig. 1. Weak enhancements of the AKR waves in a frequency range of 300 kHz to 1.0 MHz can be seen in association with the SC. The time difference between the SC onset and the start of the AKR waves is about 4 min.

frequency range from the proton cyclotron to the LHR frequencies associated with the ground-based SC onset was seen, as shown in the panel depicting the electric field component of the VLF range with a banded structure in a frequency range of 316 Hz to 1.78 kHz. The time difference between the onset of the electrostatic whistler mode

waves in space and the SC onset on the ground revealed the propagation effects of the SC disturbances in the magnetosphere. A detailed discussion and interpretation of these propagation effects is described in another paper by Shinbori *et al.* (2003).

On the other hand, a weak AKR enhancement can be seen in the PWS data within a frequency range of 300 kHz to 1.0 MHz, starting at 0746 (UT), or approximately 5 min after the SC onset. At the same time, strong VLF waves in the whistler or LHR mode were strongly enhanced at the LHR frequency. When the frequency spectra of the enhanced AKR were analyzed in detail, a two-banded structure with a harmonic relationship was seen (Benson, 1982, 1984, 1985; Mellott *et al*., 1986; Oya, 1991). For example, the AKR spectrum at 0749:23 (UT) appeared at 165 kHz to 1145 kHz. The two frequency bands in the AKR spectrum peaked at 497 kHz and 1008 kHz. These bands exhibited a have closed relationship of fundamental and harmonic frequencies. In the present case, the intensity of the fundamental AKR was stronger than that of the second-harmonic AKR. The harmonic AKR was also identified by Hosotani *et al.* (2003) using the Akebono PWS data.

As shown in Fig. 2, the energy spectra of the low-energy electrons revealed a significant change at 0741:00 (UT). This change was closely related with the SC onset. Electron fluxes within an energy range of 100 eV to 1 keV were weakly enhanced after the end of the previous activities of the low-energy electrons at 0741:00 (UT). The electron spectra showed a variation in the peak energy about 27 s after the SC onset; namely, the characteristic energy continuously decreased from about 1 keV to 100 eV within about 4 min. The electron's flux in the energy range of 1 to 3 keV showed the abrupt termination of the previous activities around the time of the SC onset.

3.3. Time difference between the onsets of SCs and AKR enhancements

To understand the relation between the SC onset and SC-related AKR activity, we examined 162 high-latitude SC events that were observed by the Akebono satellite. To identify the SC-related AKR events, we applied the following criteria: (i) the sudden appearance of AKR waves in a wide frequency range and (ii) the sudden enhancement of AKR, which had been activated prior to the SC onset. The SC-related AKR events were searched for within a time window of -15 to $+15$ min from the ground-based SC onset. As an additional criterion, the PWS instrument onboard the Akebono satellite had to have been operational for more than 10 min after the SC onset. Out of all the SC events noted in the PWS observations performed in the polar regions (162 cases), we found 85 cases of AKR enhancement associated with a ground-based SC onset. As mentioned in Section 2, for each SC event, we used the ground-based onset time of the SC as defined at Kakioka by Shinbori *et al.* (2002). Out of these 85 cases, six examples of PWS data with dynamic spectra are shown in Fig. 3. In Fig. 3, the relationship between the onset of the SCs and the AKR enhancement (including whistler mode waves) is shown for the periods covering the SC onsets. As previously noted, two types of AKR enhancements can be seen in Fig. 3. In Fig. 3 (a) and (d), weak AKR waves that were previously activated are enhanced in association with the SC onset; in the second case, the AKR emissions suddenly appeared with the SC onset. Interestingly, SC-related AKR was accompanied by second harmonic waves in the frequency spectra in several cases. Most of the SC-related AKR shown in Fig. 3 exhibited a delay time

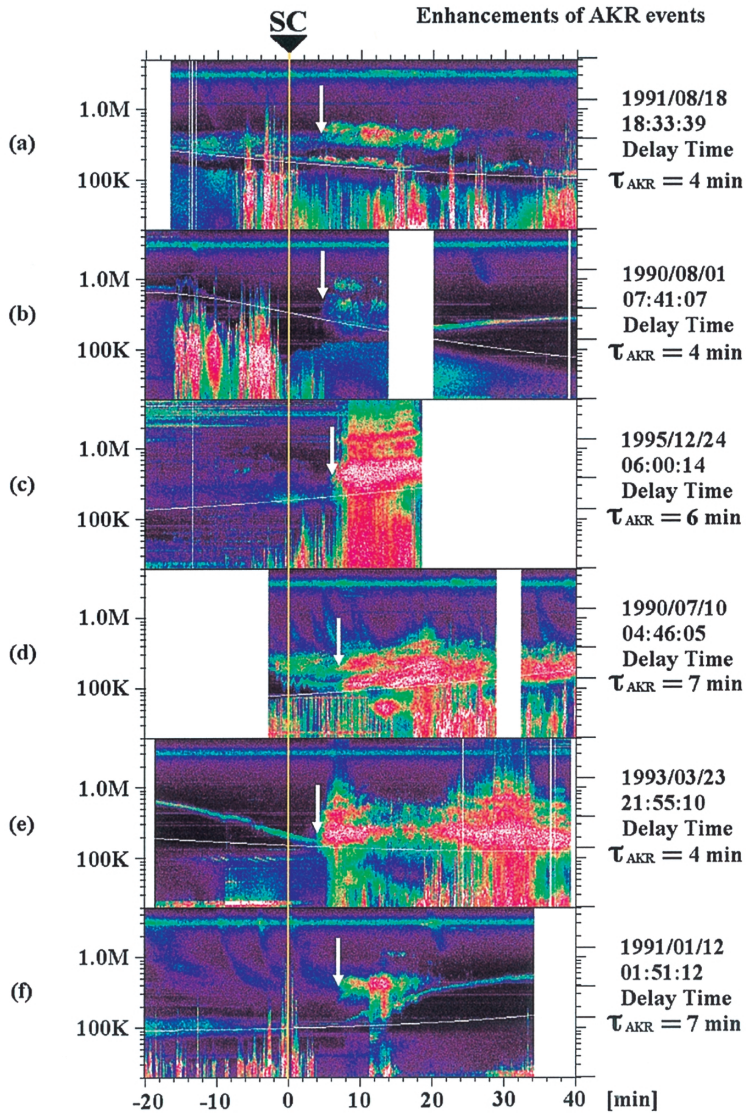

Fig. 3. Dynamic spectra of plasma waves at frequencies of 20 kHz to 5.1 MHz obtained by the PWS instruments onboard the Akebono satellite, which passed through a high-latitude region (Mlat $>45^{\circ}$). The dynamic spectra are compared with the ground-based SC onset times aligned at the same position and indicated as 'SC'. The white arrows in each panel indicate the onset time of AKR waves. The delay times of the SC-related AKR phenomena are shown on the right side of each panel in minutes.

of between 4 to 7 min after the SC onset.

In panels (d) and (f), radio emissions of solar type-III bursts that had no apparent relation with the SC onsets are shown. As it has been shown in panels (a), (b), (d) and (f), the solar type-III burst is often found in the plasma wave data from the Akebono

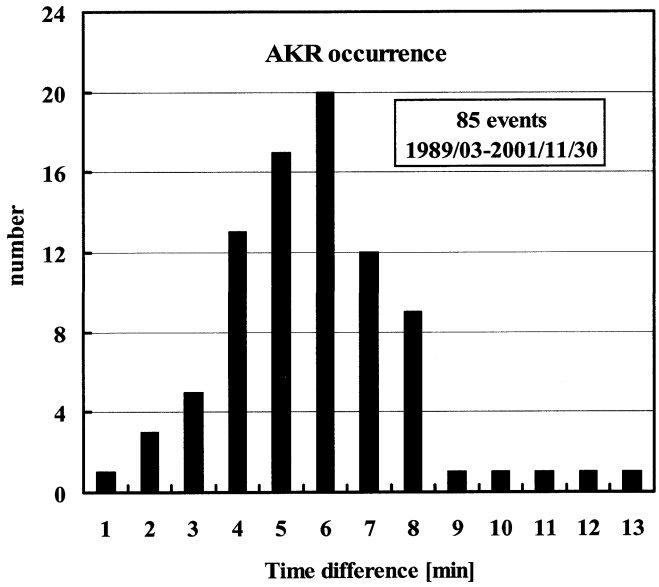

Fig. 4. Distribution of the time difference between the ground-based SC onsets and the onset of the AKR waves versus the occurrence of AKR waves. Many of these events had a time difference of between 3 to 8 min.

satellite within a period of maximum solar activity. However, the AKR phenomena can be clearly identified even in successive type III burst activity, which they appeared in a similar frequency range of dynamic spectra. Some reports have indicated that type III bursts may stimulate the onset of AKR waves (Calvert, 1981, 1985; Rosenberg *et al.*, 1995). However, within the present cases given in (d) and (f), the generation of the AKR seems to be related to the SC onsets rather than the successive arrival of type III bursts.

In Fig. 4, the delay times of the AKR enhancements after SC onset are given for the 85 events. The results in Fig. 4 show that SC-related AKR appears with a delay time in the range of 3 to 8 min, with an average delay of 5.26 min. It should be noted that the enhancement of whistler mode plasma waves triggered by the passage of the SC disturbances occurred with a time difference on the order of ten seconds (see the example of the SC triggered emissions given in Fig. 4 by Shinbori *et al.*, 2002), while the delay times for the enhancement of AKR phenomena associated with SCs are on the order of one minute.

4. Observation of SC-related THR in the polar regions

4.1. Example case observed on June 30, 1991

An example of SC-triggered plasma waves in the polar region is given in Fig. 5, which shows observations made at 4993 km (ALT), 1253 (MLT) and 78.32° (ILAT); these observations correspond to the SC onset that occurred at 0116:03 (UT). In this case, strong electrostatic whistler mode plasma waves within a frequency range of 5.12

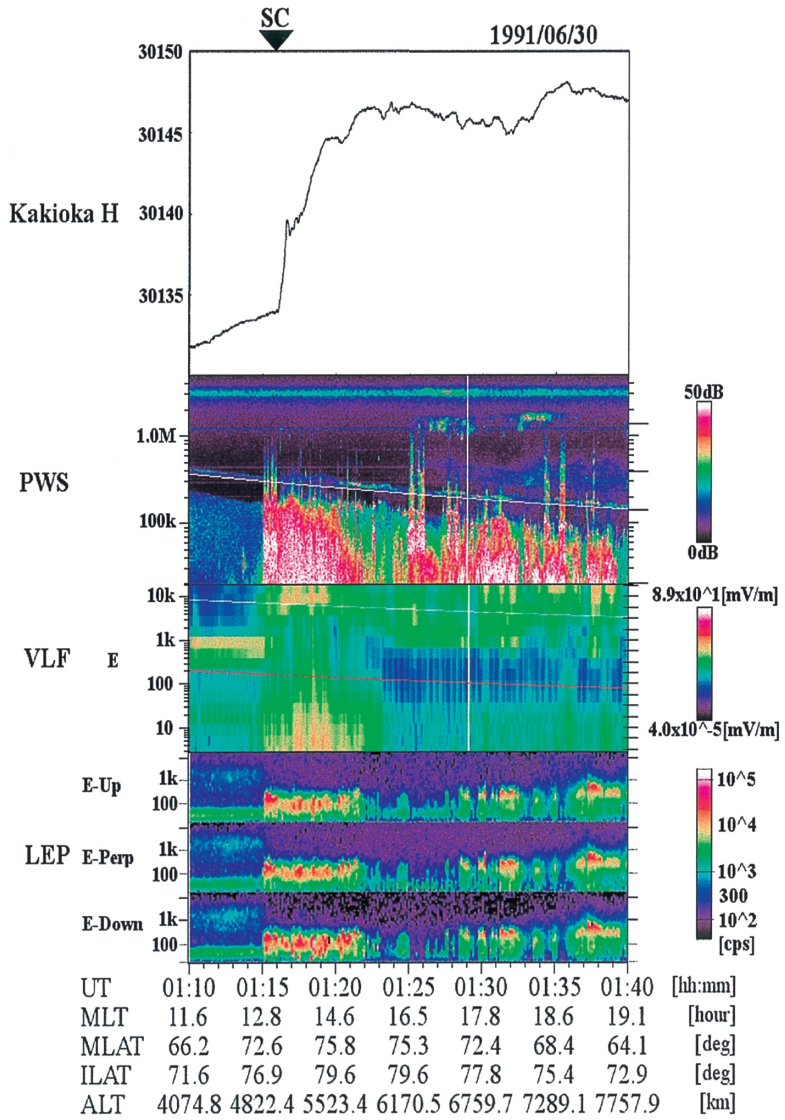

Fig. 5. An example of an SC event that occurred at 0116:03 (UT) on June 30, 1991, when the Akebono satellite passed through the dayside polar region. The formats are the same as in Fig. 1. The enhancement of THR waves in a frequency range of 900 kHz to 3.7 MHz can be seen in association with the SC. The time difference between the onsets of the SC and the THR waves was about 8 min.

kHz to 230 kHz had already been initiated at 0115:03 (UT), with a lead time of 60 s based on the SC onset time recorded by the Kakioka magnetogram. The strong electrostatic whistler mode waves were associated with the enhancement of low-energy particle fluxes. In this case, the electric field intensity of the electrostatic whistler mode waves almost reached the saturation level of the PWS receiver.

In the PWS data, THR emissions appeared within a frequency range of 900 kHz to 3.73 MHz at 0124 (UT), approximately 8 min after the SC onset. The SC-related THR continued for more than 20 min in this case.

When we analyzed the THR spectra in detail, the SC-related THR exhibited a two-banded emission structure. A one-banded structure was found within a frequency range of 900 kHz to 1.78 MHz, with a peak intensity occurring at about 1.3 MHz. Another banded structure was seen within a frequency range of 2.98 MHz to 3.73 MHz, with a peak intensity occurring at about 3.4 MHz. In this case, the frequency band width of the THR near 1.3 MHz was almost the same as that of the THR near 3.4 MHz. In this dynamic spectrum, a weak AKR enhancement within a frequency range of 250 kHz to 600 kHz was also found, simultaneous with the start of the THR associated with the SC disturbance. These facts suggest that both AKR and THR are generated by the precipitation of auroral keV electrons, which is possibly triggered by SC disturbances.

When we examined the LEP data for the observation period shown in Fig. 5, enhanced electron fluxes were found at 0115:00 (UT) within an energy range of 20 eV to 500 eV for all three pitch-angle bins. In this case, the downward electron fluxes were more intense than the upward electron fluxes. Although these electron flux enhancements corresponded with the generation of the electrostatic whistler mode waves, the relation between the AKR and THR enhancements is not clear.

4.2. Time difference between SC onsets and THR enhancement

The detail of SC-related THR enhancements were examined for SC events that occurred in the polar regions. To identify SC-related THR, we used the following criteria: (i) the THR spectra suddenly intensified within a time range of -15 min to 15 min from the onset of the SCs in the Kakioka magnetogram data and (ii) the Akebono satellite was operational for more than 30 min after the onset of the SCs. Within the 162 observation intervals, we found 19 cases of THR enhancements that occurred after ground-based SC onsets. From these 19 cases, six examples of the dynamic spectra are shown in Fig. 6, where the relationships between the SC onsets and THR enhancements (including the AKR component in the high-frequency range of more than 383 kHz) are indicated on the right side of each panel from (a) to (f). The 19 SC-related THR events can be divided into three groups. First, eight events occurred near 1.3 MHz after the SC onset as shown in panels (e) and (f). Second, six events took place near 3.4 MHz, as shown in panel (d). Finally, five events took place near 1.3 MHz and 3.4 MHz after the onset of the ground-based SC as shown in panels (a), (b) and (c). Of note, the frequency of the SC-related THR sometimes increased or decreased as a function of time, as shown in panel (f). More than 80% of the SC-related THR events had a delay time in the range of 1 to 9 min after the ground-based SC onset time.

The time differences between the THR onset and the SC onsets are given in Fig. 7. The results in Fig. 7 show that the majority of SC-related THR occurred within a delay time ranging from 1 to 9 min, with an average of 5.84 min. Considering the small number of THR events, the SC-related THR appears to have almost the same characteristics as AKR, with respect to the delay time.

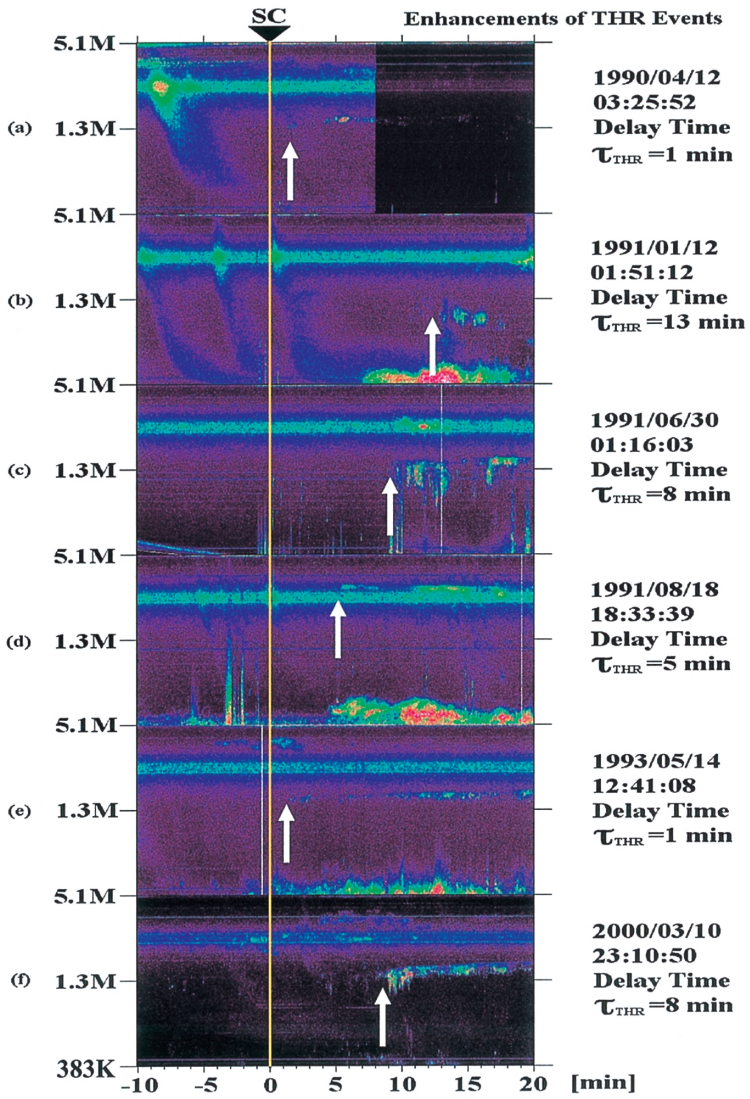

Fig. 6. Dynamic spectra of plasma waves at frequencies of 383 kHz to 5.1 MHz obtained by the PWS instruments onboard the Akebono satellite, which passed through a high-latitude region (Mlat $>45^{\circ}$). The dynamic spectra are compared with the ground-based SC onset times aligned at the same position and indicated as 'SC'. The white arrows in each panel indicate the onset time of the THR waves. The delay times of the SC-related THR phenomena is shown on the right side of each panel in minutes.

5. Discussion

5.1. AKR phenomena triggered by SCs

The results of a case study reported by Gail and Inan (1990) show that the

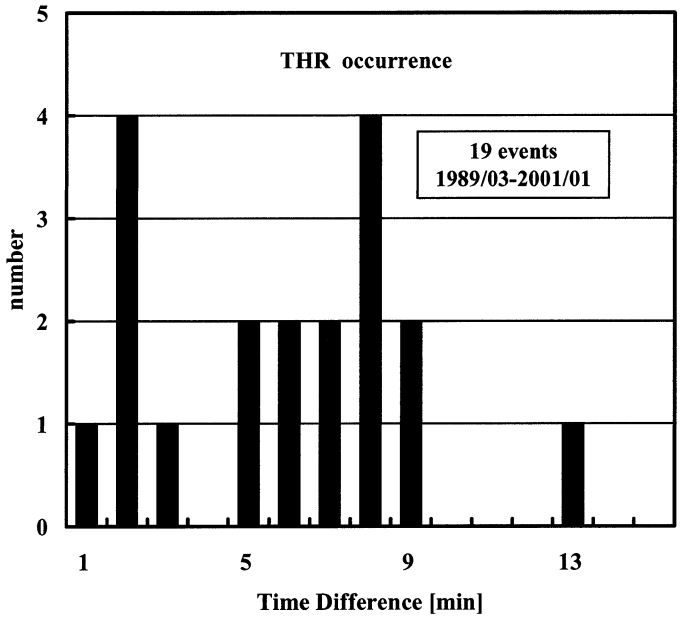

Fig. 7. Distribution of the time difference between the ground-based SC onsets and the onset of the THR waves versus the occurrence of THR waves. Many of these events had a time difference of between 1 to 9 min.

enhancement of AKR seems to start approximately 2 to 5 min after the enhancement of whistler mode waves associated with SCs. They proposed that an SC may trigger an intermediate process, such as the energization and precipitation of tail particles into the auroral region, that is, a prerequisite for AKR generation. The present study clearly shows AKR enhancements that are revealed to SC onset within a frequency range of 100 kHz to 1.2 MHz and with a delay time of approximately 2 to 8 min, with an average delay time of 5.26 min after the SC onsets. This average delay time of about 5 min between the onset of AKR in space and the SC on the ground provides some indication of the features involved in the onset of SC-triggered substorms. Kokubun *et al.* (1977) showed that energetic particle injection from the plasma sheet can be observed using the OGO-5 satellite, which was located near the midnight sector 3 min after a ground-based SC onset. From this evidence, we can conclude that these plasma sheet particles are further accelerated to keV energy in the acceleration region in the polar ionosphere. Thus, the AKR is generated by these keV electrons (Green *et al.*, 1979). As some studies on the generation of SC-triggered substorms have shown, Iyemori and Tsunomura (1983) found a delay time of about 10 min and regarded this delay as the result of propagation effects in the magnetosphere, based on the analysis of Pi2 data. They also pointed out the possibility of plasma sheet compression by the SC. Wilken *et al.* (1986) proposed that the hydromagnetic waves generated by the encounter of solar wind shock waves and the magnetopause may affect the distribution of the magnetospheric particles and fields produced by the compression. This redistribution may provide suitable conditions for the generation of a substorm, or may even actively

trigger a substorm. Ullaland *et al.* (1993) reported a delay time of about 5 min between the SC onset and the start of energetic electron precipitation into the midnight auroral regions. As a generation mechanism for SC-triggered substorms, they also proposed the idea of ballooning mode instability, caused by ion pressure anisotropy.

Therefore, as a candidate generation mechanism for the onset of SC-related AKR, magnetic disturbances associated with an SC may propagate from the dayside magnetosphere to the nightside tail region and compress the plasma sheet. As a result, ballooning mode instability, proposed by Ullaland *et al.* (1993), would first occur in this region. Later, this instability would cause current wedge disruption (proposed by Chao *et al.*, 1977; Lui, 1991), which can only occur near the earth (<15 Re), triggering the injection of plasma sheet particles into the auroral accreditation region.

To explain the considerable delay time in the AKR onset observed by the Akebono satellite, we compared our data with the auroral electrojet (AE) indices. For some events (panels (a) and (b) of Fig. 3), the variation in AE shows a simultaneous enhancement with the onset of the SC-related AKR; however, the AKR events in panels (d), (e) and (f) do not show a clear correspondence between the AE index and AKR activities. Thus, further investigation is needed to explain the delay in the AKR onset.

5.2. THR phenomena triggered by SCs

THR was previously studied by Oya *et al.* (1985) and Oya (1990); however, a detailed analysis on the occurrence frequency and the dependence of this phenomenon on magnetic activity, such as substorms or SCs, has not been made. The present study clearly shows that 19 THR events within a frequency range of about 900 kHz to 4 MHz were revealed to SC onsets. SC-related THR appeared with a delay time in the range of 1 to 9 min, with an average delay time of 5.84 min. This delay time for SC-related THR is similar to that of AKR. This similarity in delay time suggests that auroral particles associated with the SC disturbances are also involved in the generation of THR waves. However, as shown in Fig. 6, some THR events were not accompanied by AKR waves. Thus, the THR and AKR generation mechanisms may differ. The generation of SC-related THR will be examined in future studies.

6. Conclusion

Plasma wave phenomena associated with SCs have been analyzed using the database of Akebono satellite observations that has been growing since March 1989. Among the plasma wave data for 263 events, 85 cases of SC-related AKR events were found within a frequency range of 100 kHz to 1.2 MHz. The majority of the SC-related AKR spectra exhibited a two-banded structure with a harmonic relationship. The delay time between the onset of the AKR and SC tends to range between 3 and 8 min, with an average delay time of 5.26 min. From the results of the delay time analyses, magnetic disturbances associated with the SC are thought to propagate from the dayside magnetosphere to the nightside tail region and compress the plasma sheet. First, ballooning mode instability may occur in association with the magnetic compression of the plasma sheet in this region. Later, current wedge disruption, which only occurs near the earth (<15 Re), may be caused by this instability, triggering the injection of

plasma sheet particles into the auroral accreditation region. On the other hand, 19 THR events appeared within a frequency range of 900 kHz to 4 MHz after the onset of the SCs. Most of the SC-related THR spectra exhibited intense narrow-band structures with different characteristics from those reported by Oya *et al.* (1990). The delay time between the THR and SC onsets was 1 to 9 min with an average delay time of 5.84 min. These results suggest that not only SC-related AKR, but also SC-related THR may be generated as a result of SC-triggered disturbances. Future studies will investigate the occurrence characteristics, source regions and generation mechanism of THR in detail using multi-satellite observations.

Acknowledgments

The Akebono satellite was constructed and launched by the Institute of Space and Astronautical Science (ISAS). The authors thank Prof. T. Mukai and Dr. Y. Kasahara for providing the LEP and VLF data sets and for their valuable advice and comments. The magnetic field database was obtained from the WDC-C2 program at Kyoto University.

The editor thanks Dr. K. Hashimoto and another referee for their help in evaluating this paper.

References

Akasofu, S.-I. and Chao, J.K. (1980): Interplanetary shock waves and magnetospheric substorms. Planet. Space Sci., **28**, 381–385.

Araki, T. (1994): A physical model geomagnetic sudden commencement. Solar Wind Sources of Magnetospheric Ultra-Low-Frequency Waves, ed. by M.J. Engebretson *et al.* Washington, D.C., AGU, 183–200 (Geophys. Monogr. Ser., Vol. 81).

Baumjohann, W. (1986): Some recent progress in substorm studies. J. Geomagn. Geoelectr., **38**, 633–651.

Benson, R.F. (1982): Harmonic auroral kilometric radiation of natural origin. Geophys. Res. Lett., **9**, 1120–1123.

Benson, R.F. (1984): Ordinary mode auroral kilometric radiation with harmonics observed by ISIS 1. Radio Sci., **19**, 543–550.

Benson, R.F. (1985): Auroral kilometric radiation: Wave modes, harmonics and source region density structures. J. Geophys. Res., **90**, 2753–2784.

Burch, J.L. (1972): Precondition for the triggering of polar magnetic substorms by storm sudden commencements. J. Geophys. Res., **77**, 5629–5632.

Calvert, W. (1981): The stimulation of auroral kilometric radiation by type III solar radio bursts. Geophys. Res. Lett., **8**, 1091–1094.

Calvert, W. (1985): Auroral kilometric radiation triggered by type II solar radio bursts. Geophys. Res. Lett., **12**, 377–380.

Chao, J.K., Kan, J.R., Lui, A.T.Y. and Akasofu, S.-I. (1977): A model for thinning of the plasma sheet. Planet. Space Sci., **25**, 703–710.

Gail, W.B. and Inan, U.S. (1990): Characteristics of wave-particle interactions during sudden commencements 2. spacecraft observations. J. Geophys. Res., **95**, 139–147.

Gail, W.B., Inan, U.S., Helliwell, R.A., Carpenter, D.L., Krishnaswamy, S., Rosenberg, T.J. and Lanzerotti, L.J. (1990): Characteristics of wave-particle interactions during sudden commencements 1. Ground based observations. J. Geophys. Res., **95**, 119–137.

Green, J.L., Gurnett, D.A. and Hoffman, R.A. (1979): A correlation between auroral kilometric radiation and inverted V electron precipitation. J. Geophys. Res., **84**, 5216–5222.

Gurnett, D.A. (1974): The Earth as a radio source: Terrestrial kilometric radiation. J. Geophys. Res., **79**, 4227–4238.

Hayashi, K., Kokubun, S. and Oguti, T. (1968): Polar chorus emission and worldwide geomagnetic variation. Rep. Ionos. Space Res. Jpn., **22**, 149–160.

Hirasawa, T. (1981): Effects of magnetospheric compression and expansion on spectral structure of ULF emission. Mem. Natl Inst. Polar Res., Spec. Issue, **18**, 127–151.

Hosotani, A., Ono, T., Iizima, M. and Kumamoto, A. (2003): Second harmonics of auroral kilometric radiations observed by the Akebono satellite. Adv. Polar Upper Atmos. Res., **17**, 146–154.

Iyemori, T. and Rao, D.R.K. (1996): Decay of the Dust field of geomagnetic disturbance after substorm onset and its implication to storm-substorm relation. Ann. Geophys., **14**, 608–618.

Iyemori, T. and Tsunomura, S. (1983): Characteristics of the association between an SC and a substorm onset. Mem. Natl Inst. Polar Res., Spec. Issue, **26**, 139–148.

Joselyn, J.A. and Tsurutani, B.T. (1990): A note on terminology: Geomagnetic sudden impulses (SIs) and storm sudden commencements (SSCs). EOS, Trans. AGU, **71** (47), 1808–1809.

Kasahara, Y., Hosoda, T., Mukai, T., Watanabe, S., Kimura, I., Kojima H. and Niitsu, R. (2001): ELF/VLF waves correlated with transversely accelerated ions in the auroral region observed by Akebono. J. Geophys. Res., **106**, 21123–21136.

Kawasaki, K., Akasofu, S.-I., Yasuhara, F. and Meng, C.-I. (1971): Storm sudden commencements and polar magnetic substorm. J. Geophys. Res., **76**, 6781–6789.

Kimura, I., Hashimoto, K., Nagano, I., Okada, T., Yamamoto, M., Yoshino, T., Matsumoto, H., Ejiri, M. and Hayashi, K. (1990): VLF observations by the Akebono (EXOS-D) satellite. J. Geomagn. Geoelectr., **42**, 459–478.

Kokubun, S., McPherron, R.L. and Russell, C.T. (1977): Triggering of substorms by solar wind discontinuity. J. Geophys. Res., **82**, 74–86.

Lui, A.T.Y. (1991): A synthesis of magnetospheric substorm models. J. Geophys. Res., **96**, 1849–1856.

Mellott, M.M., Huff, R.L. and Gurnett, D.A. (1986): DE-1 observations of harmonic auroral kilometric radiation. J. Geophys. Res., **91**, 13732–13738.

Morozumi, H.M. (1965): Enhancement of VLF chorus and ULF at the time of SC. Rep. Ionos. Space Res. Jpn., **19**, 371–374.

Morozumi, H.M. (1966): Sudden decrease of VLF chorus intensity at the time of SC and SI. Rep. Ionos. Space Res. Jpn., **20**, 326–328.

Mukai, T., Kaya, N., Sagawa, E., Hirahara, M., Miyake, W., Obara, T., Miyaoka, H., Machida, S., Yamagishi, H., Ejiri, M., Matsumoto, H. and Itoh, T. (1990): Low energy charged particle observations in the "auroral" magnetosphere: first results from the Akebono (EXOS-D) satellite. J. Geomagn. Geoelectr., **42**, 479–496.

Oya, H. (1991): Studies on plasma and plasma waves in the plasmasphere and auroral particle acceleration region, by PWS onboard the EXOS-D (Akebono) satellite. J. Geomagn. Geoelectr., **43**, Suppl., 369–393.

Oya, H., Morioka, A. and Obara, T. (1985): Leaked AKR and terrestrial hectometric radiations discovered by the plasma wave and planetary plasma sounder experiments on board the Ohzora (EXOS-C) satellite-instrumentation and observation results of plasma wave phenomena. J. Geomagn. Geoelectr., **37**, 237–262.

Oya, H., Morioka, A., Kobayashi, K., Iizima, M., Ono, T., Miyaoka, H., Okada, T. and Obara, T. (1990): Plasma wave observation and sounder experiments (PWS) using the Akebono (EXOS-D) satellite-instrumentation and initial results including discovery of the high altitude equatorial plasma turbulence. J. Geomagn. Geoelectr., **42**, 411–422.

Rosenberg, T.J., Singh, S., Wu, C.S., LaBelle, J., Treumann, R.A., Inan, U.S. and Lanzerotti, L.J. (1995): Coincident bursts of auroral kilometric radiation and VLF emissions associated with a type III solar radio noise event. J. Geophys. Res., **100**, 281–288.

Scheildge, J.P. and Siscoe, G.L. (1970): A correlation of the occurrence of simultaneous sudden magnetospheric compressions and geomagnetic bay onsets with selected geophysical indices. J. Atoms. Terr. Phys., **32**, 1819–1830.

Shinbori, A., Ono, T. and Oya, H. (2002): SC-triggered plasma waves observed by the Akebono satellite in the

polar region and the plasmasphere. Adv. Polar Upper Atmos. Res., **16**, 126–135.
Shinbori, A., Ono, T., Iizima, M., Kumamoto, A. and Oya, H. (2003): SC related plasma waves observed by the Akebono satellite in the polar regions and inside the plasmasphere region. submitted to J. Geophys. Res.
Tepley, L.R. and Wentworth, R.C. (1962): Hydromagnetic emissions, X-ray bursts and electron bunches, 1, Experimental results. J. Geophys. Res., **67**, 3317–3333.
Ullaland, S.L., Wilhelm, K., Kangas, J. and Rieder, W. (1970): Electron precipitation associated with a sudden commencement of a geomagnetic storm. J. Atoms. Terr. Phys., **32**, 1545–1553.
Wilken, B., Baker, D.N., Higbie, P.R., Fritz, T.A., Olson, W.P. and Pfitzer, K. A. (1986): Magnetospheric configuration and energetic particle effects associated with a SSC: A case study of the CDAW 6 event on March 22, 1979. J. Geophys. Res., **91**, 1459–1473.
Wilson, G.R., Burke, W.J., Maynard, N.C., Huang, C.Y. and Singer, H.J. (2001): Global electrodymamics observed during the initial and main phase of the July 1991 magnetic storm. J. Geophys. Res., **106**, 24517–24539.